# NEW COMPACT TRIPLE-MODE RESONATOR FILTER WITH EMBEDDED INDUCTIVE AND CAPACITIVE CROSS COUPLING

**Jen-Tsai Kuo[1, *], Tsu-Wei Lin[2], and Shyh-Jong Chung[2]**

[1]Department of Electronic Engineering, Chang Gung University, Taoyuan, Taiwan

[2]Institute of Communications Engineering, National Chiao Tung University, Hsinchu, Taiwan

**Abstract**—Two new compact planar triple-mode resonators embedded with inductive or capacitive cross coupling are proposed for bandpass filter design. Both resonators consist of a shorted half-wave ring. In the first resonator, two shorted half-wave sections with inductive coupling are connected to the shorted via of the ring. In the second, two quarter-wave sections with capacitive coupling are connected. The inductive coupling is realized by a short grounded high-impedance segment, and the capacitive coupling is implemented by an interdigital capacitor. When both the inductive and capacitive coupling coefficients are properly realized, a transmission zero can be created at designated position in either upper or lower stopband. The shorted ring is accommodated inside the area of the other two resonance sections so that a compact area can be achieved. As compared with a conventional dual-mode ring resonator filter, the proposed resonators use only 46.7% and 22.5% in area. Two triple-mode resonator bandpass filters are fabricated and measured to validate the ideas. Measurement results have good agreement with the simulation responses.

## 1. INTRODUCTION

Bandpass filters are one of the key devices in the RF front end of a microwave communication system. In bandpass filter design, as compared with single-mode resonators, multimode resonators are attractive due to their compact circuit areas and improved frequency

selectivity. The simplest form of multimode resonator is the dual-mode resonator, and it has been well investigated in many publications, e.g., [1–4].

Recently, planar multimode resonator filters have been a hot research topic, especially resonators with three or more modes [5–16]. Stepped-impedance resonators (SIRs) are good candidates for the multimode purpose. Usually, impedance ratio of the high- to low-impedance segment of such a SIR is quite large. When strong or extraordinary input/output coupling is applied, a bandpass filter with a wide or ultra-wideband bandwidth can be achieved [5, 6]. A broadband filter of ninth-order can be synthesized by a cascade of three triple-mode SIRs through proper interstage coupling [7]. In [8], based on a triple-mode SIR, two extra short-circuited stubs lead the fourth resonance mode to decrease and work together with the first three resonant modes to form a quadruple-mode resonator. In [9], by properly selecting the geometric parameters and designing the input/output coupling structure, the SIRs are feasible to realize multiband multimode filters. Using a single SIR, a dual-mode dual-band, a dual-mode triple-band or a hybrid dual-/triple-mode dual-band bandpass filter can be realized.

Stub-tapped half-wave resonators are the second approach for implementing multimode resonators. The tapped open-stub plays two roles in filter design: one is perturbation for the multimode operation and the other is generation of transmission zero in the stopband [10]. In [11], a quasi-elliptic function passband is achieved by attaching a T-type open stub to the center of a three-mode SIR, which is a folded T-type stub-loaded resonator.

The third technique for devising multimode resonators is based on resonating rings. Perhaps the simplest form of a triple-mode ring is that in [12], where a diagonal trace is added to a dual-mode square ring. In [13], the triple-mode resonator is formed by modifying an open-ring resonator with a pair of open-ended coupled lines loaded with a stub-tapped section. The resonator in [14] is developed by introducing two branch lines bridging a closed-loop ring. Varying the branch line positions effectively controls the second and third resonant frequencies. In [15], a pair of coupled rings with two open stubs symmetrically tapped to the inner ring is devised to form a quadruple-mode resonator. In [16], a new triple-mode resonator is implemented by three half-wave rings shorted with a common ground via.

In this paper, two triple-mode resonators with embedded inductive and capacitive cross coupling are proposed for use in trisection filters to create a zero in the upper or lower stopband. Transmission zeros are beneficial for enhancing the rejection levels in the stopband of

a bandpass filter [17, 18]. Section 2 briefly describes the theoretical background of a trisection filter with designated zero position. Section 3 investigates resonance characteristics of the devised triple-mode resonators. Section 4 synthesizes the triple-mode resonator bandpass filters based on coupling matrix theory in Section 2, and presents the measured responses and compares with simulation. Finally, Section 5 draws the conclusion.

## 2. THEORY OF TRISECTION FILTERS

For the coupling scheme in Fig. 1, the dark circles represent resonating nodes, and empty circles stand for the source and load. The solid lines denote direct coupling, and the dash line means cross coupling between resonators 1 and 3. The corresponding $(n+2) \times (n+2)$ coupling matrix ($n$ = number of resonators) can be written as

$$[M] = \begin{bmatrix} 0 & M_{S1} & 0 & 0 & 0 \\ M_{S1} & B_1 & M_{12} & M_{13} & 0 \\ 0 & M_{21} & B_2 & M_{23} & 0 \\ 0 & M_{31} & M_{23} & B_3 & M_{3L} \\ 0 & 0 & 0 & M_{3L} & 0 \end{bmatrix} \tag{1}$$

where $M_{12}$ and $M_{23}$ will be realized by inductive coupling in our design, i.e., $M_{12} > 0$ and $M_{23} > 0$, while the cross coupling $M_{13}$ can be inductive or capacitive. The coupling between the source to the first resonator and the load to the last resonator are the input/output coupling denoted as $M_{S1}$ and $M_{3L}$, respectively. The terms $B_1$, $B_2$ and $B_3$ represent the susceptances of the three asynchronously tuned resonators. The transmission and reflection responses can be obtained as follows [19, 228–229]:

$$S_{21} = -2j[A]_{n+2,1}^{-1} \tag{2}$$

$$S_{11} = 1 + 2j[A]_{11}^{-1} \tag{3}$$

where

$$[A] = [M] + \Omega_L[U] - j[q]. \tag{4}$$
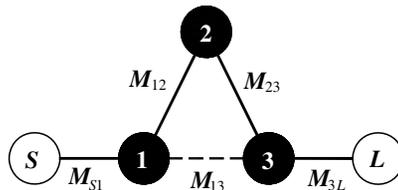


**Figure 1.** Coupling scheme of a trisection bandpass filter.

where $[U]$ is an $(n+2) \times (n+2)$ identity matrix except for $[U]_{11} = [U]_{n+2,n+2} = 0$, $[q]$ is an $(n+2) \times (n+2)$ zero matrix except for $[q]_{11} = [q]_{n+2,n+2} = 1$, $\Omega_L$ denotes the frequency variable of the lowpass prototype, and $[A]_{ik}^{-1}$ means the $(i,k)$-entry of the inverse matrix of $[A]$.

The transmission zero can be obtained by enforcing $S_{21}(\Omega_L) = 0$, leading to

$$\Omega_z = -B_2 + \frac{M_{12}M_{23}}{M_{13}} \tag{5}$$

The zero can be allocated in the upper and lower stopband when $\Omega_z$ is positive and negative, respectively. For simplicity, the magnitude of $B_2$ is assumed to be negligible and the proposed triple-mode resonator filters are designed symmetric, i.e., $M_{12} = M_{23}$ and $M_{S1} = M_{3L}$.

## 3. PROPOSED TRIPLE-MODE RESONATOR

Figure 2 shows the generic structure of the proposed microstrip triple-mode resonator. The center bottom of the inner half-wave ring is shorted to ground through short high-impedance sections and a ground via, modeled by inductors $L_{h1}$ and $L_v$, respectively. The two side arms can be half-wave sections, with inductive coupling $L_v + L_{h2}$ at their ends as shown on the top of Fig. 2. In this case, $C = \infty$. Alternatively, the two side arms can also be quarter-wave sections with capacitive coupling modeled by $C$ and in this case $L_v + L_{h_2} = \infty$. Basically, if all coupling elements are removed from the structure, the entire triple-mode resonator consists of three single-mode resonators with identical resonant frequencies. The circuit prototype for developing the triple-mode resonator can be referred to Fig. 1(a) of [16]. Here the central half-wave ring is allocated inside the traces of the other two resonating segments, leading to a compact area.
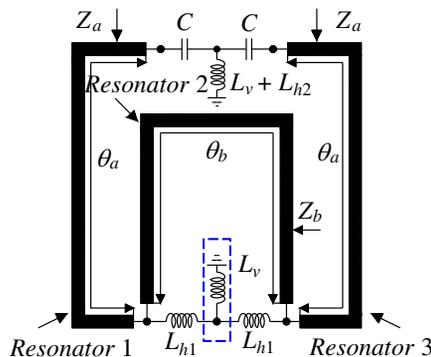


**Figure 2.** Generic structure of the proposed triple-mode resonator.

## 3.1. Resonator with Embedded Inductive Cross-coupling

Since $|B_2|$ is assumed negligible, the sign of $\Omega_z$ can be solely determined by that of $M_{12}M_{23}/M_{13}$. As shown in Fig. 2, the coupling $M_{12}$ and $M_{23}$ are inductive and positive. Note that resonators 1 and 3 are coupled with $L_v$ as well as the coupling T-network on the top. Adjustability of the coupling by $L_v$, however, will be limited by diameter of the ground via. Fig. 3(a) shows the layout of the triple-mode resonator with inductive cross-coupling, i.e., $M_{13} > 0$, implemented by series connection of a short high-impedance section $L_{x2}$ and a ground via. The equivalent inductance values for these inductive elements can be extracted.    Resonators 1 and 3 are implemented by SIRs for stopband extension and size reduction [16]. Here, the impedance ratio $R = Z_2/Z_1 = 3$ and electrical length ratio $u = \theta_2/(\theta_1 + \theta_2) = 0.67$ are



(a)



(b)
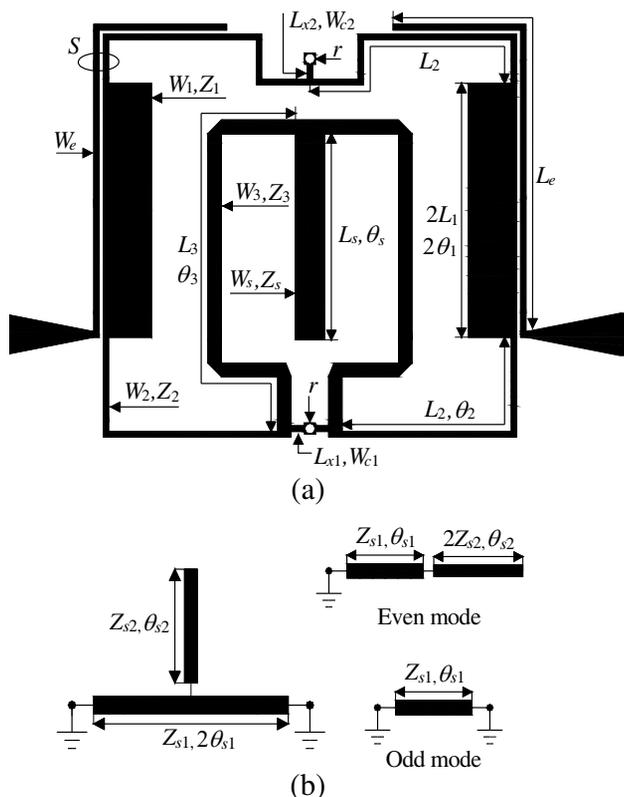
**Figure 3.** (a) Layout of the proposed triple-mode resonator embedded with inductive cross coupling. (b) The loaded stub structure with the even and odd mode equivalent circuits.

selected. For operation at 2.4 GHz, the following parameters are used:
$Z_1 = 45.3\,\Omega$, $Z_2 = 136\,\Omega$, $\theta_1 = 20.5°$, and $\theta_2 = 41.6°$.

On the opposite side of the ground via, the central ring is loaded
with a low impedance stub to fit its size into the outer closed loop.
The circuit analysis can be performed by the half circuits obtained by
bisecting the circuit with shorted and open circuit planes in the middle
as shown in Fig. 3(b). The fundamental mode resonates at 2.4 GHz
is the even mode. The parameters can be selected as $Z_s = 62.4\,\Omega$,
$\theta_s = 29.5°$, $Z_3 = 95\,\Omega$, and $\theta_3 = 62.4°$ The area of the proposed
resonator is only 46.2% of that of a conventional dual-mode ring
resonator [1].

Figure 4(a) examines the transmission response of the circuit in
Fig. 3(a) with weak input/output coupling by employing the simulation
software package IE3D [20]. It is done by setting $L_e = 0$ and leaving
a small gap of size 0.1 mm between the input/output excitations and
the resonator. The substrate has $\varepsilon_r = 2.2$ and thickness $h = 0.508$ mm
Three resonant peaks, $f_{p1}$, $f_{p2}$ and $f_{p3}$, and one transmission zero
$f_z$ in the upper stopband can be observed. The variations of the
three resonant modes and the zero versus the changes of $L_{x1}$ and $L_{x2}$
are plotted in Fig. 4(b). When $L_{x1}$ is varied from 0.2 mm to 0.8 mm
($L_{x2} = 0.4$ mm), the resonances $f_{p1}$ and $f_{p2}$ shift to lower frequencies,
but the zero $f_z$ moves to higher frequency and $f_{p3}$ is almost unchanged.
When $L_{x2}$ is varied from 0.2 mm to 0.8 mm ($L_{x1} = 0.5$ mm), $f_{p1}$, $f_{p3}$
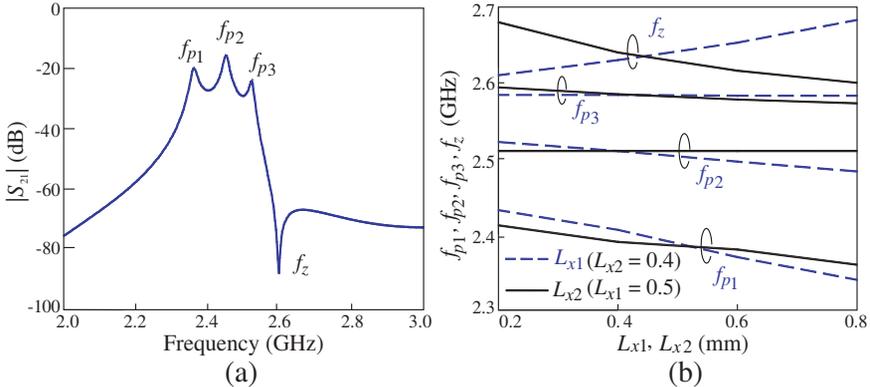


**Figure 4.** (a) Transmission response of Fig. 3(a) with $L_e = 0$.
(b) Resonant frequencies and transmission zero position versus $L_{x1}$ and
$L_{x2}$. $W_{c_1} = W_{c_2} = 0.2$ mm, radius of via hole $r = 0.2$ mm. Parameters:
$2L_1 = 9.3$, $L_2 = 10.75$, $L_3 = 16.3$, $L_s = 6.55$, $W_1 = 1.8$, $W_2 = 0.2$,
$W_3 = 0.5$, $W_s = 1.1$, $W_{c_1} = W_{c_2} = W_e = 0.2$, $L_{x1} = 0.6$, $L_{x2} = 0.4$.
All sizes are in mm.

and $f_z$ decrease, but $f_{p2}$ keeps unchanged.

## 3.2. Resonator with Embedded Capacitive Cross-coupling

Figure 5 shows the layout of the proposed triple-mode resonator embedded with capacitive cross coupling. The central ring is again loaded with a stub for area reduction, and resonators 1 and 3 are realized by grounded quarter-wavelength sections. This circuit uses only one ground via. The capacitive cross coupling is implemented by an interdigital capacitor which overcomes the inductive coupling resulted from $L_{x1}$ and the ground via to achieve $M_{13} < 0$. The selected parameters are $Z_1 = 95\,\Omega$, $\theta_1 = 90°$ (including the interdigital capacitor), $Z_s = 70.2\,\Omega$, $\theta_s = 24.7°$, $Z_2 = 95\,\Omega$, and $\theta_2 = 86.5°$. The size of the entire resonator is only 22.5% of that of a conventional dual-mode ring.

The transmission response of Fig. 5 with $L_e = 0$ is shown in Fig. 6(a). Three resonant peaks $f_{p1}$, $f_{p2}$, and $f_{p3}$ and one zero $f_z$ in the lower stopband can be observed. The variations of the three resonant frequencies and the zero against the changes of $L_{x1}$ and number of fingers $m$ of the interdigital capacitor are investigated in Fig. 6(b). When the number of fingers is increased from 2 to 6, $f_{p2}$ and $f_{p3}$ shift to lower frequencies but $f_{p1}$ is almost unchanged. When $m = 4$ and $L_{x1}$
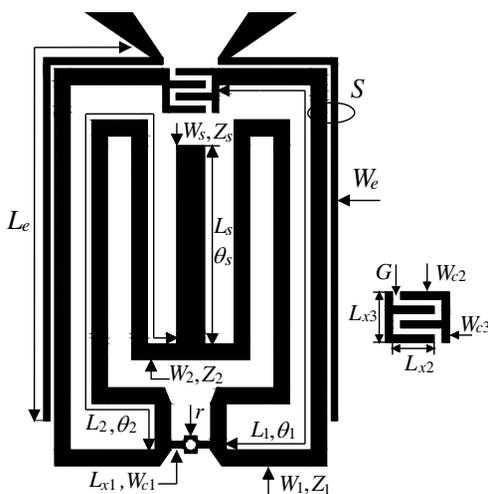


**Figure 5.** Layout of the triple-mode resonator with capacitive coupling. $L_1 = 18$, $L_2 = 22.6$, $L_s = 6.4$, $W_1 = W_2 = 0.5$, $W_s = 0.9$, $W_{c_1} = 0.2$, $L_{x1} = 0.35$, $W_{c_2} = W_{c_3} = 0.2$, $L_{x2} = 1.05$, $L_{x_3} = 1.6$, $G = 0.15$, $r = W_e = 0.2$, $L_e = 15.5$. All sizes in mm.
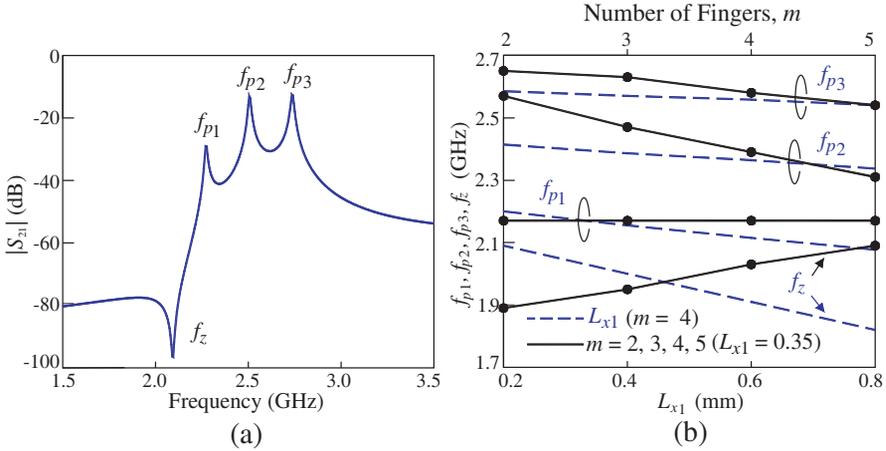
**Figure 6.** (a) Transmission response of Fig. 5 with $L_e = 0$. (b) Resonant frequencies and transmission zero frequency versus $L_{x1}$ and number of interdigital fingers $m$. Substrate: $\varepsilon_r = 2.2$, thickness $h = 0.508\,\mathrm{mm}$.

is varied from $0.2\,\mathrm{mm}$ to $0.8\,\mathrm{mm}$, $f_z$ moves up to higher frequencies, $f_{p1}$ and $f_{p2}$ shift to lower frequencies, but $f_{p3}$ is almost unchanged.

## 4. SYNTHESIS, SIMULATION AND MEASUREMENT

### 4.1. Triple-mode Resonator Bandpass Filter I

The two demonstrated filters are designed on an RT/Duroid 5880 substrate with $\varepsilon_r = 2.2$ and thickness $= 0.508\,\mathrm{mm}$ to have center frequency $f_c = 2.4\,\mathrm{GHz}$ and $|S_{11}| = -15\,\mathrm{dB}$ in the passband. The first circuit has a transmission zero at $\Omega_z = 1.406$ and fractional bandwidth $\Delta = 8.3\%$. The frequency response shown in Fig. 7 can be obtained by synthesis with the following coupling matrix [19, 279–295]:

$$[M] = \begin{bmatrix} 0 & 0.831 & 0 & 0 & 0 \\ 0.831 & 0.031 & 0.597 & 0.371 & 0 \\ 0 & 0.597 & -0.446 & 0.597 & 0 \\ 0 & 0.371 & 0.597 & 0.031 & 0.831 \\ 0 & 0 & 0 & 0.831 & 0 \end{bmatrix} \quad (6)$$

To obtain $[M]$ in (6), first determine the transmission zero $\Omega_z$ with (5). If $\Omega_z > 0$, the zero is in the upper stopband. If the zero is designated in the lower stopband, then $\Omega_z$ should be negative. Then, enforce $|S_{11}| = -15\,\mathrm{dB}$, or other specified value, in (3). Next, find the

matrix entries by solving simultaneous equations derived from (1) and (2). Finally, some entries might need fine tuning for enhancing the input matching.

The elements in matrix $[M]$ in (6) are values in the lowpass domain. In the bandpass domain, the external quality factor ($Q_{ext}$)
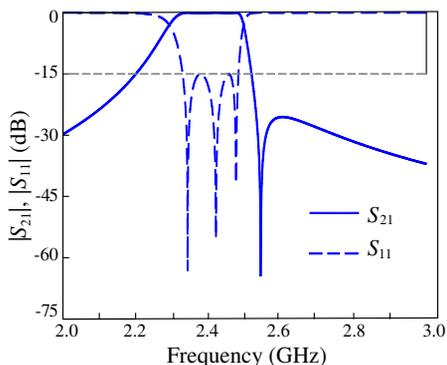


**Figure 7.** Frequency response synthesized by coupling matrix (6).
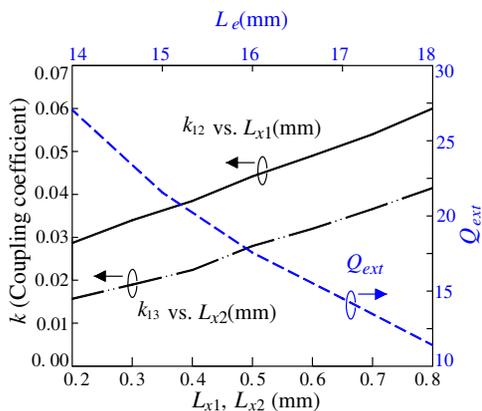


**Figure 8.** Design graphs: change of $k_{12} = k_{23}$ versus $L_{x1}$ with $L_{x2} = 0.55$ mm, variation of $k_{13}$ against $L_{x2}$ with $L_{x1} = 0.5$ mm and dependence of $Q_{ext}$ on $L_e$. Parameters: $2L_1 = 9.3$, $L_2 = 10.75$, $L_3 = 16.3$, $L_s = 7.55$, $W_1 = 1.8$, $W_2 = 0.2$, $W_3 = 0.5$, $W_s = 1.1$, $W_{c_1} = W_{c_2} = W_e = 0.2$, $L_{x1} = 0.5$, $L_{x2} = 0.55$, $S = 0.15$, $r = 0.2$, $L_e = 16.4$. All sizes are in mm.

can be calculated from $M_{S1} = M_{3L}$:

$$Q_{ext} = \frac{1}{\Delta \times M_{S1}^2} \qquad (7)$$

Likewise, the coupling coefficients $k_{ij}$ between resonators $i$ and $j$ can be calculated by

$$k_{ij} = M_{ij} \times \Delta \qquad (8)$$

Figure 8 shows variations of $k_{ij}$ versus $L_{x1}$ and $L_{x2}$ and changes of $Q_{ext}$ versus $L_e$. The extraction method of $k_{ij}$ and $Q_{ext}$ can be referred to [21]. Since all coupling between the resonators are inductive, both $k_{12}$ and $k_{23}$ increase when either $L_{x1}$ or $L_{x2}$ is increased. In addition, $Q_{ext}$ becomes smaller, when the length of feed-line ($L_e$) increases. Based on (6), the coupling coefficients in the bandpass domain $k_{12} = k_{23} = 0.0495$, $k_{13} = 0.0308$, and $Q_{ext} = 17.44$ are required. The corresponding $L_{x1}$, $L_{x2}$, and $L_e$ can be obtained from these plots.



(a)

(b)



(c)
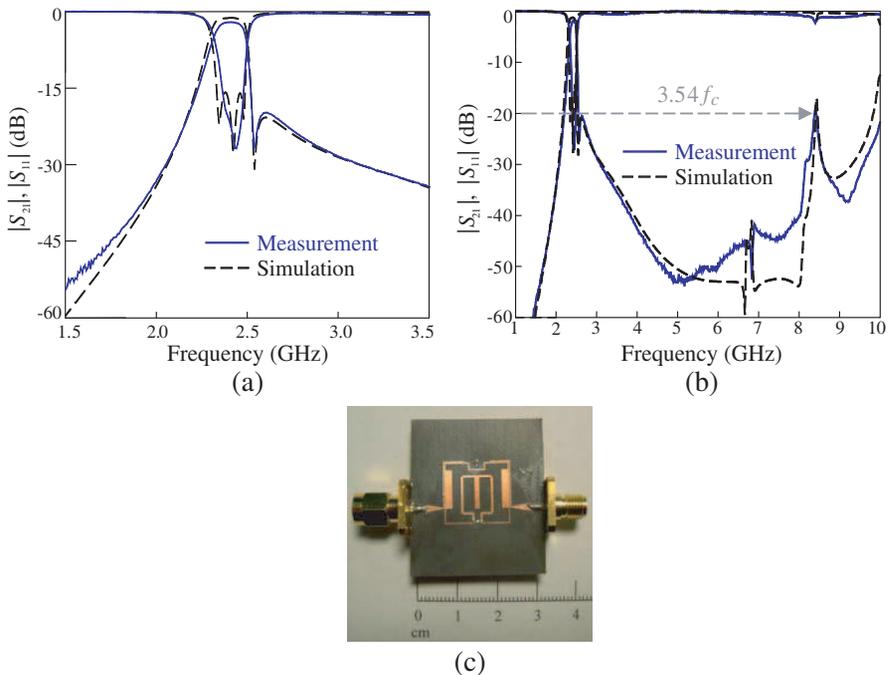
**Figure 9.** Simulated and measured responses of the first proposed triple-mode filter in (a) $1.5 \sim 3.5\,\text{GHz}$ and (b) $1 \sim 10\,\text{GHz}$. (c) Photograph of the measured circuit. All sizes are given in Fig. 8.

Figure 9(a) compares the measured and simulated in-band responses of the fabricated circuit. The measured data indicate that $|S_{21}| = -1.78$ dB at $f_c$ and $\Delta = 7.93\%$. The transmission zero is at $2.55$ GHz. Fig. 9(b) shows the performance of the filter from 1 to 10 GHz. The upper stopband with a 20-dB rejection is extended to $3.54 \times f_c$. Such good rejection performance is resulted from the use of the SIRs [3]. Measured responses show good agreement with the simulation results. Fig. 9(c) shows the photograph of the measured circuit.
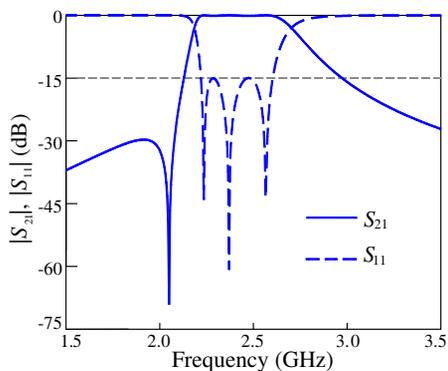


**Figure 10.** Frequency response synthesized by coupling matrix (9).
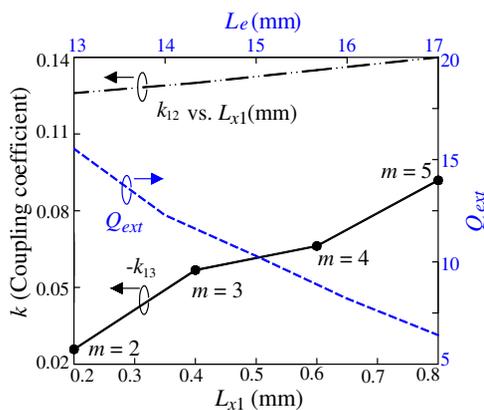


**Figure 11.** Design graphs: change of $k_{12} = k_{23}$ versus $L_{x1}$ with $m = 4$ and $W_{c1} = 0.2$ mm, variation of $-k_{13}$ against $m$ with $L_{x1} = 0.35$ mm and $W_{c2} = 0.2$ mm, and dependence of $Q_{ext}$ on $L_e$. All sizes are given in Fig. 5.

## 4.2. Triple-mode Resonator Bandpass Filter II

The second triple-mode bandpass filter is synthesized to have a transmission zero with $\Omega_z = -2.11$ and $\Delta = 15\%$. The frequency response in Fig. 10 can be obtained by the following coupling matrix:

$$[M] = \begin{bmatrix} 0 & 0.975 & 0 & 0 & 0 \\ 0.975 & -0.116 & 0.854 & -0.439 & 0 \\ 0 & 0.854 & 0.452 & 0.854 & 0 \\ 0 & -0.439 & 0.854 & -0.116 & 0.975 \\ 0 & 0 & 0 & 0.975 & 0 \end{bmatrix} \tag{9}$$

The negative cross coupling coefficient $M_{13}$ is implemented by capacitive coupling. Fig. 10 shows variations of $k_{12}$ and $-k_{13}$ against $L_{x_1}$ and change of $Q_{ext}$ versus $L_e$. From (9), the coupling coefficients are $k_{12} = k_{23} = 0.128$, $k_{13} = -0.0658$, and $Q_{ext} = 7.01$. Based on the
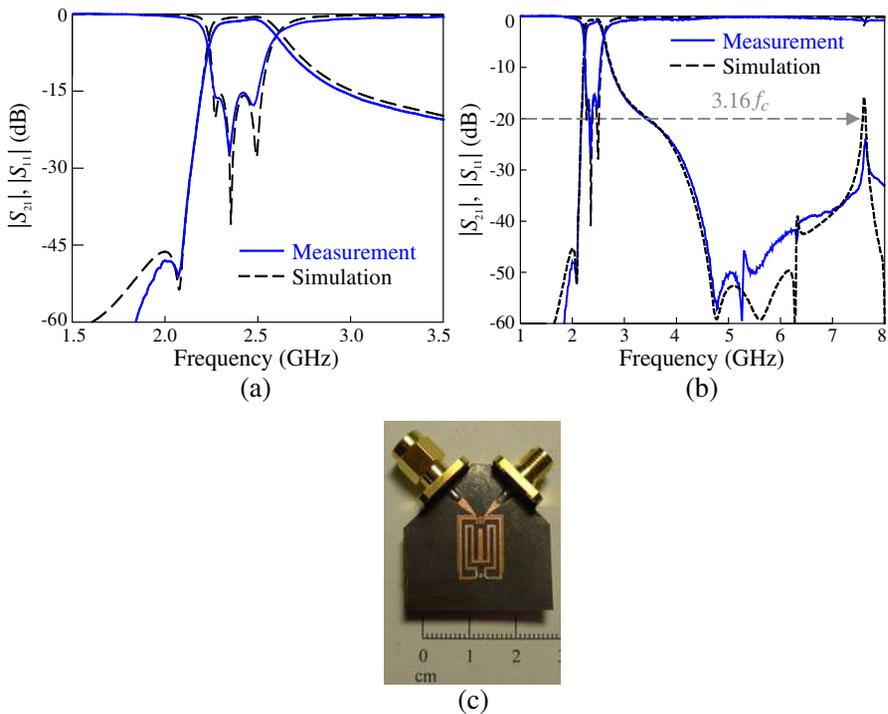


Figure 12. Performance of the triple-mode resonator bandpass filter with capacitive cross coupling. (a) $1.5 \sim 3.5\,\mathrm{GHz}$ and (b) $1 \sim 8\,\mathrm{GHz}$. (c) Photograph of the measured circuit. All circuit geometric parameters are in Fig. 5.

plots in Fig. 11, values of $L_{x_1}$, $m$ (number of fingers), and $L_e$ to meet the design specifications can be determined.

Figure 12(a) shows the simulation and measured responses of the second demonstrated triple-mode bandpass filter. The measured $\Delta = 14.3\%$, in-band insertion loss $= 1.28\,\mathrm{dB}$ and $f_z = 2.07\,\mathrm{GHz}$. Fig. 12(b) shows the comparison in a band from 1 to 8 GHz. The measured responses match well with the simulation data. The upper stopband with 20-dB rejection is at $3.16\,f_c$, which is very close to the second resonant frequency of the shorted quarter-wave sections. Fig. 12(c) shows the photograph of the measured filter.

## 5. CONCLUSION AND DISCUSSION

Two triple-mode resonators are devised with embedded inductive or capacitive cross coupling for designing trisection filters with a transmission zero in the upper and lower stopbands. The cross coupling, including sign and magnitude, is determined by a coupling matrix for synthesizing a trisection filter with a designated transmission zero. Since short-circuited half-wave rings and quarter-wave sections are used, the triple-mode resonators occupy less than one half or one quarter of the circuit area of a traditional dual-mode ring. Measurement data show good agreement with simulation results.

As shown in the generic structure in Fig. 2, the proposed triple-mode resonator is composed of three single-mode resonators. On the other hand, as shown in Fig. 3(a), these three resonators are tied up together, so that the whole structure can also be treated as a single resonator with three resonances. The three peaks of the transmission responses in Fig. 4(a) and Fig. 6(a) demonstrate this idea. If the whole structure is treated as a "single resonator," then it is a triple-mode ring resonator. The configuration incorporates the design of resonating elements and appropriate inter-resonator coupling, including magnitude and type (capacitive or inductive), for synthesis of a trisection filter with transmission zero designated in upper or lower stopband. The proposed configuration is very flexible and can be extended to multiple-mode ring resonator structure or higher-order designs [22], where a quintuple-mode ring resonator is demonstrated.

## REFERENCES

1. Kundu, A. C. and I. Awai, "Control of attenuation pole frequency of a dual-mode microstrip ring resonator bandpass filter," *IEEE Trans. Microw. Theory Tech.*, Vol. 49, No. 6, 1113–1117, Jun. 2001.

2. Wei, C.-L., B.-F. Jia, Z.-J. Zhu, and M.-C. Tang, "Design of different selectivity dual-mode filters with E-shape resonator," *Progress In Electromagnetics Research*, Vol. 116, 517–532, 2011.

3. Kuo, J.-T. and C.-Y. Tsai, "Periodic stepped-impedance ring resonator (PSIRR) filter with a miniaturized area and desirable upper stopband characteristics," *IEEE Trans. Microw. Theory Tech.*, Vol. 54, No. 3, 1107–1112, Mar. 2006.

4. Chen, C.-H., C.-S. Shih, T.-S. Horng, and S.-M. Wu, "Very miniature dual-band and dual-mode bandpass filter designs on an integrated passive device chip," *Progress In Electromagnetics Research*, Vol. 119, 461–476, 2011.

5. Zhu, L., S. Sun, and W. Menzel, "Ultra-wideband (UWB) bandpass filters using multiple-mode resonator," *IEEE Microw. Wireless Comp. Lett.*, Vol. 15, No. 11, 796–798, Nov. 2005.

6. Wang, H., Q.-X. Chu, and J.-Q. Gong, "A compact wideband microstrip filter using folded multiple-mode resonator," *IEEE Microw. Wireless Comp. Lett.*, Vol. 19, No. 5, 287–289, May 2009.

7. Chiou, Y.-C., J.-T. Kuo, and E. Cheng, "Broadband Quasi-Chebyshev bandpass filter with multimode stepped-impedance resonators (SIRs)," *IEEE Trans. Microw. Theory Tech.*, Vol. 54, No. 8, 3352–3357, Oct. 2006.

8. Wong, S. W. and L. Zhu, "Quadruple-mode UWB bandpass filter with improved out-of-band rejection," *IEEE Microw. Wireless Comp. Lett.*, Vol. 19, No. 3, 152–154, Mar. 2009.

9. Chiou, Y.-C. and J.-T. Kuo, "Planar multiband bandpass filter with multimode stepped-impedance resonators," *Progress In Electromagnetics Research*, Vol. 114, 129–144, 2011.

10. Ma, K., K. C. B. Liang, R. M. Jayasuriya, and K. S. Yeo, "A wideband and high rejection multimode bandpass filter using stub perturbation," *IEEE Microw. Wireless Comp. Lett.*, Vol. 19, No. 1, 24–26, Jan. 2009.

11. Shen, W., X.-W. Sun, and W.-Y. Yin, "A novel microstrip filter using three-mode stepped impedance resonator (TSIR)," *IEEE Microw. Wireless Comp. Lett.*, Vol. 19, No. 12, 774–776, Dec. 2009.

12. Lugo, C. and J. Papapolymerou, "Planar realization of a triple-

mode bandpass filter using a multilayer configuration," *IEEE Trans. Microw. Theory Tech.*, Vol. 55, No. 2, 296–301, Feb. 2007.

13. Srisathit, K., A. Woraphishet, and W. Surakampontorn, "Design of triple-mode ring resonator for wideband microstrip bandpass filters," *IEEE Trans. Microw. Theory Tech.*, Vol. 11, No. 58, 2867–2877, Nov. 2010.

14. Cho, C. S., J. W. Lee, and J. Kim, "Dual- and triple-mode branch-line ring resonators and harmonic suppressed half-ring resonators," *IEEE Trans. Microw. Theory Tech.*, Vol. 54, No. 11, 3968–3974, Nov. 2006.

15. Lok, U.-H., Y.-C. Chiou, and J.-T. Kuo, "Quadruple-mode coupled-ring resonator bandpass filter with quasi-elliptic function passband," *IEEE Microw. Wireless Comp. Lett.*, Vol. 18, No. 3, 179–181, Mar. 2008.

16. Lin, T.-W., J.-T. Kuo, and S.-J. Chung, "New triple-mode ring resonator bandpass filter with source-load coupling," *IEEE MTT-S Int. Microwave Symp. Dig.*, 2011.

17. Ho, M.-H. and P.-F. Chen, "Suspended substrate stripline bandpass filters with source-load coupling structure using lumped and full-wave mixed approach," *Progress In Electromagnetics Research*, Vol. 122, 519–535, 2012.

18. Kuo, J.-T. and S.-W. Lai, "New dual-band bandpass filter with wide upper rejection band," *Progress In Electromagnetics Research*, Vol. 123, 371–384, 2012.

19. Cameron, R. J. M., C. M. Kudsia, and R. R. Mansour, *Microwave Filters for Communication Systems*, Wiley, New Jersey, 2007.

20. Zeland Software, Inc., *IE3D Simulator*, Jan. 1997.

21. Hong, J.-S., *Microstrip Filters for RF/Microwave Applications*, Wiley, New Jersey, 2011.

22. Lin, T.-W., J.-T. Kuo, and S.-J. Chung, "Bandpass filter with generalized multiple-mode ring resonator configuration," *IEEE MTT-S Int. Microw. Symp. Dig.*, 2012.